RSC Advances

ROYAL SOCIETY OF CHEMISTRY

www.rsc.org/advances

Spectrin-like domain 2 of DRP2 serves as a novel binding region for the NLS2 and 3 sub-domains of L-periaxin

Yan Yang[1,2] , YaWei Shi[1*]

[1]Key Laboratory of Chemical Biology and Molecular Engineering of the Ministry of Education, Institute of Biotechnology, Shanxi University, Taiyuan 030006,China

[2] Chemical and Biological Engineering College, Taiyuan University of Science and Technology, Taiyuan 030006, China

Running title: L-periaxin possesses an unusual nuclear localization signal

*To whom correspondence should be addressed: Ya Wei Shi, Institute of Biotechnology, Shanxi University, Wucheng Road 92, Taiyuan 030006, P. R.China, Tel.: 0086-351-7018268; Fax: 0086-351-7018268; E-mail address: yaweishi@ sxu. edu.cn

Keyword: L-periaxin; DRP2; NLS domain; spectrin-like domain

Background: The interaction of L-periaxin with DRP2 provides signal transduction and nutritional factor transportation in PNS.

Results: NLS1 domain involved in nucleo-cytoplasmic shuttling, NLS2-3 participated in interaction with spectrin-like domain2 of DRP2.

Conclusion: NLS domain of L-periaxin ensures nuclear targeting and links extracellular matrix proteins to cytoskeleton.

Significance: Binding model of DRP2 and L-periaxin is crucial for understanding the role of L-periaxin in PNS.

FOOTNOTES

* This work was supported by the Natural Science Foundation of China (Grant No. 31170748).

[1] To whom correspondence should be addressed: Institute of Biotechnology,Shanxi University, Wucheng Road 92, Taiyuan, 030006, P.R. China. Tel.: 0086-0351-7018208; Fox: 0086-0351-7018208; E-mail: yaweishi@sxu.edu.cn

[2] The abbreviations used are: DRP2, dystroglycan-dystrophin-related proteins; NLS, nuclear-localization-signal; CMT, Charcot-Marie-Tooth; EPPD, ezrin-periplakin-periaxin-desmoyokin; PDZ, PSD-95/Discs Large/ZO-1; NES, nuclear export signal; LMB, LeptomycinB; PNS, peripheral nervous system; PDG, L-periaxin-DRP2-dystroglycan; EGFP, enhanced green fluorescent protein; YFP, yellow fluorescent protein; RFP, red fluorescent protein; GST, glutathione S-transferase; BiFC, Bimolecular fluorescence complementation; Co-IP, Co-Immunoprecipitation; DAPI, 2-(4-Amidinophenyl)-6-indolecarbamidine dihydrochloride; FITC, fluorescein isothiocyanate.

ABSTRACT

L-periaxin is an important scaffolding protein that is expressed in Schwann cells and lens fiber cells. In Schwann cells, loss or mutation of the *PRX* gene disrupts compact peripheral myelin and causes severe demyelination neuropathy. DRP2 is the only reported protein to interact with periaxin to form the L-periaxin-DRP2-dystroglycan (PDG) complex, which can provide structural and signaling functions by linking the extracellular matrix to the Schwann cell cytoskeleton. In this report, the interaction between L-periaxin and DRP2 was further investigated by bimolecular fluorescence complementation (BiFC), GST pull-down, CO-IP, and Fluorescence spectroscopy. Results demonstrated that spectrin-like domain 2 of DPR2 played a critical role in the complex of DRP2 and L-periaxin. Furthermore, the DRP2 spectrin-like domain 2 only interacted with the NLS2 and NLS3 sub-domains in L-periaxin. These data revealed a previously unknown binding model between DRP2 and L-periaxin.

Periaxin is a cytoskeletal-associated protein that was initially identified in myelinating Schwann cells (1). Based on its localization and the demyelination neuropathy phenotype associated with the gene knockout mouse model, periaxin has been confirmed to play an essential role in peripheral nerve myelination, and the mutations of the *periaxin (PRX)* gene cause Charcot-Marie-Tooth (CMT) 4F, an autosomal recessive demyelinating disease (2-5). Periaxin has been also reported in cytoskeletal complexes of lens fibers. On the lens intracellular face, L-periaxin interacts with ezrin, periplakin, and desmoyokin, which comprise a macromolecular complex of EPPD; moreover, L-periaxin plays a key role in cell adhesive interactions (6).

PRX, which encodes two periaxin isoforms, namely, L-periaxin and the truncated S-periaxin, has been mapped to chromosome 19q13.13-q13.2 (3, 4, 5, 7). Both proteins are identical in the N-terminal PDZ (PSD-95/Discs Large/ZO-1) protein-binding domain; besides the PDZ domain, L-periaxin can be further divided into the basic nuclear localization signal (NLS) region, a long-repeat domain, and C-terminal acidic domain (4, 7). L-periaxin is a 147 kDa protein with 1461 amino acid residues, whereas S-periaxin is a 16 kDa protein with 147 amino acid residues (7).

The PDZ domain is an important protein-protein interaction motif that is implicated in the assembly of macromolecular signaling complexes (8). The PDZ domain of L-periaxin contains a nuclear export signal (NES) between residues 73 and 86 that allows it to shuttle from the nucleus to the cytoplasm, and the nuclear export activity of L-periaxin can be inhibited by NES mutation (L83/Q, L85/Q) or by LMB (LeptomycinB) treatment (9). The mutation that knocks out the PDZ domain causes barely functional, and the homodimerization of periaxin have vanished from *ΔPDZ-Prx* mice. (10). Meanwhile, in the absence of the PDZ domain, peripheral nerves show that dystroglycan-dystrophin-related protein 2 (DRP2)-periaxin-dystroglycan protein complexes (PDG) decrease in the plasma membrane of Schwann cells (10). The NLS domain of L-periaxin, and not the PDZ domain, is integrated with the PDG complex through direct interactions with DRP2 (11).

The interaction between DRP2 and L-periaxin also requires DRP2 phosphorylation (12). Unlike L-periaxin, DRP2 is not a component of Schmidt-Lanterman incisures in the peripheral nervous system (PNS) (13). At six-month-old *Prx* null mice, myelin-specific profiles, such as myelin-associated glycoprotein, peripheral myelin protein zero (P0), and myelin basic protein, exhibit normal levels, but nerve conduction velocity reduces and causes focal hypermyelination and demyelination (14). In contrast to *Prx* null mice, *Drp2* null mice show slow and periodic demyelination or abnormal myelin regeneration (12). At nine months, the low percentage of onion bulbs in *Drp2* null mice is comparable with that in *Prx* null mice, which also demonstrate disrupted Cajal bands (10). The interaction of L-periaxin with DRP2 likely plays a role in cell signal transduction and nutritional factor transportation (11) Nevertheless, the coupling model of DRP2 and L-periaxin remains unclear, and the only evidence is the N-terminal of DRP2 linked to the NLS domain of L-periaxin (11).

L-periaxin has an unusual tripartite -type NLS that is composed of NLS1 (118-139 aa), NLS2 (162-175 aa), and NLS3 (183-194 aa), which localize L-periaxin to the Schwann cell

nucleus (15). DRP2 protein comprises two spectrin-like repeats (1 and 2) and WW domain in the N-terminal region and EF domain, as well as ZZ and coiled-coil domain in the C-terminal region. To explain the interactions between L-periaxin and DRP2, a series of experiments was conducted. Results indicated that L-periaxin was linked to spectrin-like domain 2 of DRP2 protein. Moreover, NLS1 of the NLS domain in L-periaxin was found to be involved in nucleo-cytoplasmic shuttling of L-periaxin protein, but both NLS2 and NLS3 participated in interaction with spectrin-like domain 2 of DRP2.

EXPERIMENTAL PROCEDURES

Plasmid construction-The *L-periaxin* (AB046840.1) was cloned into pCMV-Tag3B (Myc tagged) and named pCMV-Tag3B-*L-periaxin*. The fragments of *L-periaxin-N-1-103* (PDZ domain, 1-103 aa), *L-periaxin-N104-196* (NLS domain, 104-196 aa), *L-periaxin-M197-105*9 (repeat domain, 197-1059 aa), *L-periaxin-C1060-1461* (acidic domain, 1060-1461 aa) were generated by PCR with appropriate primer sets to generate pEGFP-*L-periaxin-N1-102*, pEGFP-*L-periaxin-N104-196*,*pEGFP-L-periaxin-M198-1059*,pEGFP-*L-periaxin-C1060-146 1*. The pEGFP vector encodes an enhanced green fluorescent protein (EGFP) which has been optimized for fluorescence localization of the fusion protein or the higher expression in mammalian cells. (Fig.1A). A similar strategy was adopted to generate His-tag expression vector, including pET-MG-*NLS*, pET-MG-*NLS1*, pET-MG-*NLS2*, and pET-MG-*NLS3*.

The full-length *DRP2* (BC111695.1), *DRP2-N1-384* (1-384 aa), and *DRP2-C385-954* (385-954 aa), as well as the different truncated fragments, such as *DRP2-N1-179* (spectrin-like domain 1, 1-179 aa) and *DRP2-N180-349* (spectrin- like domain 2, 180-349 aa), were cloned into pEGFP, pmCherry-C1 (red fluorescent protein, RFP tagged), or pGEX-6P-1 (glutathione S-transferase, GST tagged), respectively (Fig. 1A).

The construction of BiFC vectors contains the fragments *N1-155* and fragments *C156-239* from Yellow Fluorescent Protein (YFP) (16, 17). The DNA encoding *N1-155* fragment was digested with *BamHI/NotI*, inserted into pEGFP-N1, and named pYN vector, in which the EGFP tag was replaced with YFP fragmented *N1-155*. A similar strategy was used to generate the pYC vector, in which the EGFP tag was replaced with YFP fragmented *C156-239* with both *Nhe*I and *Xho*I digestion. A list of BiFC plasmids is summarized in Fig. 3A. In pYN-*NLS,* the sequences encoding *NLS* were fused to the N-terminal of pYN. A series of N-terminal of DRP2 BiFC plasmids, namely, *N1-384, N1-179*, and *N180-349*, was fused to the C-terminal of pYC and named pYC-*DRP2-N1-384*, pYC-*DRP2-N1-179*, and pYC-*DRP2-N180-349*, respectively. All the sequences were verified by DNA sequencing.

Cell culture and transfection-Rat RSC96 Schwann cells (Type Culture Collection of the Chinese Academy of Sciences, Shanghai, China) were maintained in Dulbecco's modified Eagle's medium supplemented with 10% fetal bovine serum (FBS) at 37 °C in a humidified atmosphere containing 5% CO_2. For BiFC assays, confluent HeLa cells were maintained at 37 °C with 5% CO_2 in RPMI-1640 containing 10% FBS.

The cells were seeded on sterile glass cover slips in six-well trays and cultured overnight prior to transfections. At 60%-70% confluence, the cells were transiently transfected with TurboFect transfection reagent (Thermo Scientific, United States) according to the manufacturer's instructions.

Microscopic analysis for fluorescence colocalization and BiFC-At 24 h after transfection, cells were fixed with 1 mL of Immunological Staining Fix Solution (Beyotime Institute of Biotechnology, Shanghai, China). Subsequently, cells were washed briefly in PBS (140 mM NaCl, 2.7 mM KCl, 10 mM Na_2HPO_4, 1.8 mM KH_2PO_4, pH 7.3). Cells transfected with pCMV-tag3B-*L-periaxin*/pEGFP-*DRP2-N1-384* were blocked in a solution of 5% (v/v) fetal bovine serum and 0.3% (v/v) Triton X-100 in PBS at room temperature for 1 h. and the blocked cells were incubated overnight with rabbit anti-Myc (Beyotime, Shanghai, China) and mouse anti-EGFP (Beyotime, Shanghai, China). Next, slides were washed with PBS buffer and incubated with the secondary antibodies fluorescein isothiocyanate (FITC)-labeled goat anti-mouse (Transgene, Beijing, China) and tetramethyl rhodamine isothiocyanate (TRITC)-labeled goat anti-rabbit (Transgene, Beijing, China) at room temperature. After washing, cells were stained with 1 μg/mL 4',6-diamidino-2-phenylindole (DAPI) reagent

(Solarbio, Beijing, China) for 10 min at 37 °C. Cells were subsequently examined with Delta Vision (API, USA) at 60×magnification. To the EGFP or RFP fusion proteins in the cells, such as EGFP-L-periaxin or RFP-DRP2, or the cells of BiFC, were just fixed, PBS washed and then DAPI stained. The fluorescent imaging of fixed cells were visualized using Delta Vision and the related fluorescent are measured with EGFP to FITC channel, RFP to TRITC channel. The Pearson Coefficient of Correlation were calculated, the values of Pearson Coefficient of Correlation indicates how closely the green and red fluorescence are colocalized, and the full colocalization is 1.0. BiFC fluorescent imaging response to FITC channel. All the digital images were processed with Adobe Photoshop CS2 9.0.

Flow cytometry analysis - At 24 h post-transfection, HeLa cells were maintained at 4 °C for 4 h. Cell monolayers were trypsinized and resuspended in 500 μL of PBS, followed by analysis with a FACSCalibur. Cells transfected with pYN/pYC constructs were used to set the baseline for fluorescence detection, and approximately 10,000 events were recorded from each sample.

Co-immunoprecipitation (Co-IP) and Western blot-RSC96 cells were transiently transfected with pCMV-tag3B-L-*periaxin/*pEGFP-*DRP2*,pCMV-tag3B-L-*periaxin*/pEGFP-*DRP2-N1-384*, pCMV-tag3B-L-*periaxin*/pEGFP-*DRP2-C385-954*,pCMV-tag3B-*NLS*/pEGFP-*DRP2-N1-179*, and pCMV-tag3B-*NLS*/pEGFP-*DRP2*-N180-349. After 48 h of transfection, whole cell lysates were harvested in 400 μL of lysis buffer (20 mM HEPES, pH 7.6, 150 mM NaCl, 2 mM $MgCl_2$, 10% glycerol, 0.5% Triton X-100, and 1 mM DTT plus 0.1% protease/ phosphate inhibiters). The cells were then kept on ice for 15 min and centrifuged at 4 °C. The supernatant was incubated with 2 μL of EGFP antibodies or 2 μL of mouse IgG as control and allowed to rotate overnight at 4 °C. Protein A+G Agarose (Beyotime, Shanghai, China) was added and incubated for 4 h at 4 °C, followed by washing with lysis buffer. The samples were separated by 10% SDS-PAGE gel, transferred onto a PVDF membrane (Millipore, USA), and analyzed by Western blot with corresponding antibodies.

Protein expression and purification-All the fusion proteins were expressed in *Escherichia coli* BL21. When transformed bacteria were grown to mid-log phase (OD_{600} = 0.6-0.8) in Luria-Bertani medium at 37 °C,0.3 mM isopropyl-β-D-thiogalacto-pyranoside was added overnight at 16 °C to induce expression of these fusion proteins. The cells were harvested and then lysed by sonication on ice. The supernatant was incubated with glutathione sepharose beads (GE Healthcare Life Sciences for GST fusion proteins) or nickel- nitrilotriacetic acid column (GE Healthcare Life Sciences for His fusion proteins). Furthermore, the elution product was analyzed by Sephacryl S-200 gel filtration chromatography using the same buffer (50 mM Tris-HCl, pH 8.0, 100 mM NaCl, 1 mM DTT, and 5 mM β-mercaptoethanol).

GST pull-down-GST-DRP2-N1-384, GST-DRP2-N1-179, GST-DRP2-N180-349, and an approximately equimolar amount of GST protein were each incubated with 25 μL of glutathione-sepharose 4B beads in PBS buffer (140 mM NaCl, 2.7 mM KCl, 10 mM Na_2HPO_4, 1.8 mM KH_2PO_4, pH 7.3) for 2 h at 4 °C. Beads were washed extensively with PBS buffer. The supernatant of cell lysate or purified His-tag fusion proteins was added to the pre-equilibrated beads and incubated for 2-4 h at 4 °C. Beads were washed extensively, and bound proteins were eluted with 10 mM glutathione (25 μL). The eluted proteins were analyzed by SDS-PAGE and Western blot with corresponding antibodies.

FITC-labeling NLS proteins and fluorescence spectroscopy-FITC was conjugated to recombinant NLS protein and different sub-domains of NLS1, NLS2, and NLS3 according to the manufacturer's instructions (FluoReport-FITC protein labeling, Molecular Probes). In brief, FITC was dissolved in dimethylsulfoxide, diluted with the conjugation buffer of 0.1 M $NaHCO_3$-NaOH (pH 9.0), and immediately added to protein production overnight at 4 °C in the dark (FITC/protein = 100/1). The conjugated protein was exchanged with HEPES buffer (20 mM HEPES, 100 mM NaCl, pH 7.4). The concentration of FITC-labeling peptide was calculated by Equation (1). Where protein concentration is a protein concentration of the Fluorescein-Protein conjugate; A_{280} is the actual absorbance at 280 nm of a FITC-protein; (A_{494}×0.3) is the correction factor due to the absorbance of FITC at 280 nm; α is the final dilution ratio of the labeled protein; and ε is the molar extinction coefficient of the protein at 280 nm.

$$\text{protein concentration (M)} = \frac{[A_{280} - (A_{494} \times 0.3)] \times \alpha}{\varepsilon} \quad (1)$$

The fluorescence spectra were recorded on a Perkin-Elmer LS-55 fluorescence spectrophotometer at room temperature. All measurements were performed in a total sample volume of 1 mL of HEPES buffer (20 mM HEPES, 100 mM NaCl, pH 7.4), and a 5 mm path length cuvette was used at an excitation wavelength of 494 nm, and monitoring emissions at 518nm. The titration experiment was repeated 3 times, and the titration curves were prepared by plotting (F-F0) with gradually increasing recombination protein concentration. Curves were fitted with Origin 8.0.

RESULTS

Interaction and colocalization of N1-384 of DRP2 with L-periaxin- To substantiate the interaction of periaxin with DRP2, Co-IP experiments were performed. RSC96 cells transiently transfected with pCMV-tag3B-*L-periaxin* and pEGFP-*DRP2*, and the supernatants of cell lysate were subjected to immunoprecipitation with a polyclonal EGFP antibody. For control studies, the immunoprecipitations were performed with irrelevant mouse IgG. The results revealed that EGFP-tagged DRP2 could co-precipitate Myc-tagged L-periaxin, which had an adequate size of 147 kDa (Fig. 1B). Next EGFP-tagged fragments of DRP2-N1-384 or DRP2-C385-954 were analyzed by immunoprecipitation with polyclonal anti-Myc. Fig. 1C demonstrates that the 65 kDa EGFP-DRP2-N1-384 (*lane 4*) interacts with Myc-L-periaxin, no specific binding were observed with the 90 kDa DRP2-C385-954 fragments (*lane 6)* or the negative control (*lane 3,5)*. This finding was consistent with the results of a previous study (11).

The colocalization results of pCMV-tag3B-*L-periaxin*/pEGFP-*DRP2-N1-384* also showed that DRP2-N1-384 colocalized to the cytoplasma with full length L-periaxin (Fig. 1D). These data suggested an obvious interaction between the N-terminal of DRP2 and L-periaxin.

Interaction between NLS domain of L-periaxin and spectrin-like domain 2 (N180-349) of DRP2-The N1-384 of DRP2 protein is composed of spectrin-like repeats (spectrin-like domain 1, N1-179; spectrin-like domain 2, N180-349) and the WW domain (N350-384) (Fig. 2A). To identify the contribution of various domains of L-periaxin, purified GST-DRP2-N1-384 (Fig. 2B) was used to pull down EGFP-L-periaxin-N1-103, EGFP-L-periaxin-N104-196, EGFP-L-periaxin-M197-1059, and EGFP-L-periaxin-C1060-1461. As expected, DRP2-N1-384 could pull down L-periaxin-N1-196, especially the fragment of L-periaxin-N104-196 (Fig. 2C (*lane 2*) and D (*lane 2)*). The results revealed that the NLS domain was involved in the interaction between L-periaxin and DRP2. A few difference was found in GST-DRP2-N1-384 pull down of L-periaxin-N1-196 (PDZ+NLS) compared with that of L-periaxin-NLS (Fig. 2C and 2D). L-periaxin-PDZ may help the NLS domain to bind with DRP2-N1-384.

An obvious interaction between NLS and DRP2-N180-349 was only detected by pull-down assay (Fig. 2E (*lane 2*)). No binding was detected for equivalent amounts of GST-DRP2-N1-179 or the control GST protein alone. The peptide binding data in the fluorescence spectrum also implied a significant increase in NLS domain binding of DRP2-N1-384 and DRP2-N180-349 (Fig. 2F). These experiments suggested that spectrin-like domain 2 of DRP2 (N180-349) was a critical region for NLS.

BiFC techniques were also used to test whether the interaction of DRP2-N180-349 and L-periaxin-NLS can induce fluorescence complementation in HeLa cells.

HeLa cells grown on glass coverslips were co-transfected with pYN/pYC, pYN-*NLS*/pYC-*DRP2-N1-384*, pYN-*NLS*/pYC-*DRP2-N1-179*, or pYN-*NLS*/pYC-*DRP2-N180-349*. The results showed that pYN-*NLS*/pYC-*DRP2-N1-384* induced strong BiFC fluorescence compared with pYN/pYC (Fig. 3B). Besides, pYN-*NLS*/pYC-*DRP2-N180-349* exhibited a fairly higher BiFC fluorescence than pYN-*NLS*/pYC-DRP2-*N1-179* (Fig. 3B).

Flow cytometry was used to analyze the percentage of fluorescent cells expressed in pYN/pYC, pYN-*NLS/*pYC-*DRP-N1-384*, pYN-*NLS*/pYC-*DRP2-N1-179*, and pYN-*NLS*/pYC-*DRP2-N180-349*, . The proportion of fluorescent cell from

pYN-*NLS*/pYC-*DRP2-N1-384* positive control was defined as 100%. As expected, the pYN-*NLS*/ pYC-*DRP2-N1-179* group expressed only 4% of fluorescence cells, whereas pYN-*NLS*/pYC-*DRP2-N180-349* showed an improvement and expressed approximately 80% of fluorescence cells (Fig.3C and 3D). These results further confirmed that spectrin-like domain 2 (N180-349) of DRP2 was required for the NLS domain of L-periaxin binding.

Interaction of NLS2 and NLS3 of L-periaxin with spectrin-like domain 2 (N180-349) of DRP2-The L-periaxin-NLS domain is composed of three sub-domains, namely, NLS1 (K_{118}-K_{139}), NLS2 (K_{162}-K_{175}) and NLS3 (R_{183}-R_{194}) (Fig. 4A). A series of pull-down experiments was performed to assess the NLS sub-domains capable of binding to spectrin-like domain 2 of DRP2. The results indicated that the EGFP-tagged NLS2 and NLS3 were bound to GST-DRP2-N180-349, whereas no interaction was detected between EGFP-NLS1 and GST-DRP2-N180-349 (Fig. 4B(*lane 2* and *3*)).

The L-periaxin-NLS domain was required for nuclear localization and distribution in the contact point of the RSC96 cell membrane, which was consistent with the findings on the EGFP-tagged NLS1 sub-domain (Fig. 5A and 5B). By contrast, the sub-domains of EGFP-tagged NLS2 and NLS3 localized in the cell cytoplasm (Fig. 5A and 5 B).

Intracellular destination of the NLS sub-domains were evaluated using RFP-tagged DRP2-N1-384 in RSC96 cells. The results of fluorescence analysis suggested that RFP-DRP2-N1-384/EGFP-L-periaxin, and RFP-DRP2-N1-384/EGFP-NLS were colocalized to the cytoplasm and cytomembrane (Fig. 1D and Fig. 6B). Moreover, the co-transfected results showed extensive colocalization for RFP-DRP2-N1-384 with EGFP-NLS2 and EGFP-NLS3 in the cytoplasm (Fig. 6D and 6E). In contrast, no obvious colocalization was observed for EGFP-tagged NLS1 and RFP-tagged DRP2-N1-384 (Fig. 6C). As shown by pearson correlation coefficient between the FITC and TRITC channels, the strong overlaps for EGFP-NLS, EGFP-NLS2, EGFP-NLS3 with RFP-DRP2-N1-384 had been calculated (Fig. 6B, 6D and 6E), and there is little correlation between EGFP-NLS1 and RFP-DRP2-N1-384 (Fig. 6C and 6F). These data were consistent with the interactions of DRP2 with the NLS2 and NLS3 sub-domains of L-periaxin, but the NLS1 sub-domain may be involved in nucleocytoplasmic shuttling.

DISCUSSION

L-periaxin is necessary for the stabilization and regeneration of the Schwann cell-axon unit and connection of the myelin sheath to the surrounding extracellular matrix (10, 18). Several lines of evidence indicated that the periaxin protein's function is directly related to CMT4F disease (18). According to statistical data of 18 cases of CMT4F, periaxin is predicted to generate a truncated non-function protein that is devoid of the acidic terminal domain, which is thought to be important in maintaining normal myelin formation (15, 18, 19).

An embryonic age (E) of 13.5 is the earliest time at which L-periaxin is detectable by immunocytochemistry in the nucleus (adaxonal membrane) of Schwann cells of the mouse PNS. L-periaxin has been shown to be associated with the plasma membrane of Schwann cells, and it predominately localizes at the abaxonal Schwann cell membrane (opposing the basal lamina) where it is believed to function in a signaling complex (2). The deletion of the NLS domain abrogates the nuclear uptake of L-periaxin and it is energy dependent (15). A previous study showed that the PDZ domain of L-periaxin guides its translocation from the nucleus to the cytoplasm (9). The PDZ and NLS domains may be directly correlated with the localization and functionality of L-periaxin. Although the details remain unclear, the translocation of L-periaxin to the abaxonal Schwann cell plasma membrane is assumed to be a relatively late event during myelination (11). In mature myelin, the ability of the PDZ domain of L-periaxin to homodimerize may account for the clustering of DRP2(11). The interaction of DRP2 and L-periaxin appears to be a feature of the maturation of the sheath, and the PDG complex may serve as a channel for the delivery of nutritional factors or cell signal transduction (11, 12).

In this study, spectrin-like domain 2 of DRP2 could bind to NLS2 and NLS3 of L-periaxin, but not to NLS1, which is essential for nuclear localization (Fig. 7). NLSs in

L-periaxin exhibited similar sequences, which comprised a number of basic residues, and the content of positive charge Lys and Arg was above 36% of total amino acid residues. The reason for the different binding abilities of the three NLS sub-domains in L-periaxin to DRP2 may be from the amount of positive charge. In particular, the positive charge of NLS2 and NLS3 reached 40% and 50% of total amino acid residues, respectively. By binding to the importin/karyopherin complex, NLS1 may have a direct role in regulating nuclear uptake (20). In terms of NLS2 and NLS3, interacting with DRP2 and anchoring to the Schwann cell plasma may have important significance (Fig. 7). Upon combining with different ligands, such as DRP2 (11) and ezrin (21), the protein expression, cellular localization, and biological function of L-periaxin should be affected.

DRP2, dystrophin, and utrophin constitute the vertebrate members of the dystrophin branch of the superfamily; this family has a large N-terminal extension of actin-binding CH domains and up to 24 spectrin repeats, DRP2 retains only two of the spectrin repeats(22). The spectrin-like repeats are three-helix bundle structures, which are important interaction sites for multiple structural and signaling proteins. Most aromatic residues in the hydrophobic core of spectrin-like repeats are typically conservative, and the acidic residues are predominantly distributed throughout the surface (23). In recent advances, spectrin-like repeats act as an interface for signal transduction mediation and an interactive part of membrane channels, adhesion molecules, receptors, and transporters (23). DRP2 may participate in the dynamic interaction between the spindle microtubules and kinetochore during mitotic chromosome segregation (24).

Although both spectrin-like domains 1 and 2 in DRP2 have similar sequences, only spectrin-like domain 2 plays a critical role in in interaction between L-periaxin and DRP2. This role may contribute to its slight difference in spatial structure. Future work should focus on the structure of the NLS complex in L-periaxin and spectrin-like domain 2 of DRP2.

Acknowledgments: We acknowledge that this project is supported by the Natural Science Foundation of China (Grant No. 31170748).

Conflict of interest: The authors declare that they have no conflicts of interest with the contents of this article.

Author contributions: Yan yang performed and analyzed the experiments results and wrote the paper, Yawei Shi conceived, designed, coordinated and modified the paper. All authors reviewed the results and approved the final version of the manuscript.

REFERENCES:

1. Gillespie, C., Sherman, D.L., Blair, G.E., and Brophy, P.J. (1994) Periaxin, a novel protein of myelinating Schwann cells with a possible role in axonal ensheathment. *Neuron*. 12, 497-508.
2. Scherer, S.S., Xu, Y.T., Bannerman, P.G., Sherman, D.L., and Brophy, P.J. (1995) Periaxin expression in myelinating Schwann cells: modulation by axon-glial interactions and polarized localization during development. *Development*. 121,4265-4273.
3. Gillespie, C.S., Lee, M., Fantes, J.F., and Brophy, P.J. (1997) The gene encoding the Schwann cell protein periaxin localizes on mouse chromosome 7 (Prx). *Genomics*. 41, 297-298.
4. Dytrych, L., Sherman, D.L., Gillespie, C.S., and Brophy, P.J. (1998) Two PDZ domain proteins encoded by the murine periaxin gene are the result of alternative intron retention and are differentially targeted in Schwann cells. *J Biol Chem*. 273, 5794-5800.
5. Boerkoel, C.F., Takashima, H., Stankiewicz, P., Garcia, C.A., Leber, S.M., Rhee-Morris, L., and Lupski, J.R. (2001) Periaxin mutations cause recessive Dejerine-Sottas neuropathy. *Am J Hum Genet*. 68,325-333.
6. Maddala, R., Skiba, N.P., Lalane, R., Sherman, D.L., Brophy, P.J., and Rao, P.V. (2011) Periaxin is required for hexagonal geometry and membrane organization of mature lens fibers. *Dev Biol*. 357, 179-190.
7. Delague, V., Delague, V., Bareil,C., Tuffery, S., Bouvagnet, P., Chouery, E., Koussa, S., Maisonobe, T., Loiselet, J., Mégarbané, A., and Claustres, M. (2000) Mapping of a new locus for autosomal recessive demyelinating Charcot-Marie-Tooth disease to 19q13.1-13.3 in a large consanguineous Lebanese family: exclusion of MAG as a candidate gene. *Am J Hum Genet*.67, 236-243.
8. Lee, H.J., and Zheng, J.J. (2010) PDZ domains and their binding partners: structure, specificity, and modification. *Cell Commun Signal*. 8,1-18.
9. Shi, Y., Zhang, L., and Yang, T. (2014) Nuclear export of L-periaxin, mediated by its nuclear export signal in the PDZ domain. *PLoS One*. 9, e91953.
10. Wu, L.M., Williams, A., Delaney, A., Sherman, D.L., and Brophy, P.J. (2012) Increasing internodal distance in myelinated nerves accelerates nerve conduction to a flat maximum. *Curr Biol*. 22, 1957-1961.
11. Sherman, D.L., Sherman, D.L., Fabrizi, C., Gillespie, C.S., and Brophy, P.J. (2001)Specific disruption of a schwann cell dystrophin-related protein complex in a demyelinating neuropathy. *Neuron*. 30,677-687.
12. Sherman, D.L., Wu, L.M., Grove, M., Gillespie, C.S., and Brophy, P.J. (2012) Drp2 and periaxin form Cajal bands with dystroglycan but have distinct roles in Schwann cell growth. *J Neurosci*. 32, 9419-9428.
13. Patzig, J., Jahn, O., Tenzer, S., Wichert, S.P., Monasterio-Schrader, P., Rosfa, S., Kuharev, J., Yan, K., Bormuth, I., Bremer, J., Aguzzi, A., Orfaniotou, F., Hesse, D., Schwab, M.H., Möbius, W., Nave, K.A., and Werner, H.B. (2011)Quantitative and integrative proteome analysis of peripheral nerve myelin identifies novel myelin proteins and candidate neuropathy loci. *J Neurosci*. 31,16369-16386.
14. Gillespie, C.S., Sherman, D.L., Fleetwood-Walker, S.M., Cottrell, D.F., Tait, S., Garry, E.M., Wallace, V.C., Ure, J., Griffiths, I.R., Smith, A., and Brophy, P.J. (2000)Peripheral demyelination and neuropathic pain behavior in periaxin-deficient mice. *Neuron*. 26,

523-531.
15. Sherman, D.L. And Brophy, P.J. (2000) A tripartite nuclear localization signal in the PDZ-domain protein L-periaxin. *J Biol Chem*. 275, 4537-4540.
16. Nyfeler, B., Michnick, S.W., and Hauri, H.P. (2005) Capturing protein interactions in the secretory pathway of living cells. *Proc Natl Acad Sci U S A*. 102, 6350-6355.
17. Yemei, R. and Yawei, S. (2014) Analysis of Protein Interaction Between S-periaxin by Bimolecular Fluorescence Complementation. *Chinese Journal of Cell Biology*. 8, 1060-1067.
18. Barankova, L., Sisková, D., Hühne, K., Vyhnálková, E., Sakmaryová, I., Bojar, M., Rautenstrauss, B., and Seeman, P. (2008) A 71-nucleotide deletion in the periaxin gene in a Romani patient with early-onset slowly progressive demyelinating CMT. *Eur J Neurol*. 15, 548-551.
19. Yan Y, Tingting, P., and Yawei, S. (2015) Periaxin Protein And Charcot-Marie-Tooth. *Chinese journal of biochemistry and molecular biology*.2,1-8.
20. Giraud, G., Stadhouders, R., Conidi, A., Dekkers, D.H., Huylebroeck, D., Demmers, J.A., Soler, E., and Grosveld, F.G. (2014) NLS-tagging: an alternative strategy to tag nuclear proteins. *Nucleic Acids Res*. 42, 1-12.
21. Hui, W. Yemei, R. Yinjun, D. and Yawei, S. (2014) Analysis of the Interaction between L-Periaxin and Ezrin. *Chinese Journal of Biochemistry and Molecular Biology*. 3, 279-283.
22. Jin, H., Tan,S., Hermanowski, J., Böhm ,S., Pacheco, S., McCauley, J.M., Greener, M.J., Hinits, Y., Hughes, S.M., Sharpe, P.T., and Roberts, R.G.(2007)The dystrotelin, dystrophin and dystrobrevin superfamily: new paralogues and old isoforms. *BMC Genomics*. 8,1-19.
23. Ipsaro, J.J., Huang, L., and Mondragon, A. (2009) Structures of the spectrin-ankyrin interaction binding domains. *Blood*. 113, 5385-5393.
24. Si-pin, T., Xianzhong, X., and Roberts, R.G. (2008) Identification of a dystrophin-related protein 2(DRP2) associating protein by yeast two hybridization. *China Journal of Modern Medicine*. 18,133-137.

FIGURE LEGENDS

FIGURE 1. Interaction of L-periaxin and DRP2 in RSC96 cells. A. Schematic of L-periaxin and DRP2. Amino acid residues in each domain are numbered on top of the diagram. B. Verification of the interaction between L-periaxin and DRP2 by Co-IP assay. RSC96 cells were transfected with the indicated plasmids for 48 h. Lysates were subjected to Co-IP with mouse IgG or anti-EGFP and then analyzed by Western blot with anti-EGFP and anti-Myc. C. Verification of the interaction between L-periaxin and DRP2-N1-384 by Co-IP assay. The groups of DRP2-N1-384 (lane 1) and C385-954 (lane 2) were used as input; lanes 3 and 5 were the negative control of mouse IgG; lanes 4 and 5 were immunoprecipitated with Myc antibody. D. Subcellular localization of L-periaxin (pCMV-tag3B-*L-periaxin*) and DRP2-N1-384 (pEGFP-*DRP2-N1-384*). At 24 h post-transfection, cells were fixed, stained with DAPI, probed with rabbit anti-Myc and mouse anti-EGFP, incubated with the secondary antibodies of FITC goat anti-mouse and TRITC goat anti-rabbit. The image with Delta Vision at 60× magnification , and analyzed with POL, DAPI, FITC and TRITC channel, scale bar = 10 μm.

FIGURE 2. Interaction between NLS domain of L-periaxin and spectrin-like domain 2 of DRP2. A. Schematic of L-periaxin and DRP2. Amino acid residues of each domain are numbered on top of the diagram. B. Purification of GST-tagged truncated DRP2 and His-tagged NLS of L-periaxin. C. Verification of the interaction between the different domains of L-periaxin and DRP2-N1-384 by GST pull-down assay. EGFP-tagged N1-196, M197-1059, and C1060-1461 protein lysates are shown in the input lane. GST control (lane C) or GST-DRP2-N1-384 (lane 1-4) was incubated with RSC96 cell lysate and detected by Western blot with EGFP antibody. D. EGFP-tagged N1-103 and 104-196 were incubated with GST control (lane C) or GST-DRP2-N1-384 (lane 1-2), and the interaction between the NLS and DRP2-N1-384 was analyzed by GST pull down. E. Verification of the interaction between His-L-periaxin-NLS and GST-DRP2-N180-349 by GST pull down. F. Fluorescence quenching analysis of the interaction between L-periaxin-NLS and DRP2-N1-384, N1-179, N180-349. NLS protein is conjugated to FITC. The curves shows the fluorescence intensity by plotting (F-F0) with gradually increasing DRP2-N1-384 protein concentration in HEPES buffer (20 mM HEPES, 100 mM NaCl, pH 7.4). Results represent the means of 3 independent experiments.

FIGURE 3. DRP2-N180-349 interaction with L-periaxin-NLS assayed by BiFC. A. Schematic of BiFC fusion proteins used in this study. B. BiFC assay to evaluate interactions between L-periaxin and DRP2. HeLa cells grown on glass coverslips were co-transfected with pYN-*NLS*/pYC-*DRP2-N1-384*, pYN-*NLS*/pYC-*DRP2-N1-179*, and pYN-*NLS*/pYC-*DRP2-N 180-349*, and pYN/pYC was used as the control. At 24 h post-transfection, cells were fixed, analyzed with FITC fluorescence, and imaged with Delta Vision at 60× magnification. Scale bar=10μm. C. Flow cytometry analysis of the fluorescent percentage of BiFC. D. Quantitative analysis of the fluorescent percentage of BiFC (3 independent experiments, * $p \leq 0.05$).

FIGURE 4. Interaction of DRP2 and L-periaxin-NLS2 and NLS3. A. Schematic of the NLS sub-domains used in GST pull-down assay. B. EGFP-tagged NLS1, NLS2, and NLS3 expressed in RSC96 cells were pulled down with GST control (C) and GST-DRP2-N180-349(lane 1-3). Bound proteins were probed with anti-EGFP or anti-GST antibodies as indicated. One-tenth of the lysates were run as input.

FIGURE 5. Localization of L-periaxin, L-periaxin-NLS, and different sub-domains of NLS in RSC96 cells. A. RSC96 cells were transfected with the plasmid pEGFP-*L-periaxin*, pEGFP-*NLS*, *NLS1*, *NLS2*, and *NLS3*. Cells were then analyzed with FITC channel (for EGFP) and DAPI channel (for nucleus), imaged with Delta Vision at 60× magnification. Scale bar=10 μm. B. Histogram of positions of 100 cells. The gray "N" indicates the nucleus, and the black "C" shows the location of the cytoplasm.

FIGURE 6. Colocalization of DRP2-N1-384 with L-periaxin-NLS or sub-domains of NLS

in RSC96 cells. A-E. RSC96 cells were co-transfected with EGFP/RFP, EGFP-NLS/RFP-DRP2-N1-384, EGFP-NLS1/RFP-DRP2-N1-384, EGFP-NLS2/RFP-DRP2-N1-384, and EGFP-NLS3/RFP-DRP2-N1-384. Images were observed with Delta Vision at 60× magnification, and analyzed with DAPI, FITC and TRITC channel, scale bar=10 μm. The scatter plot of the colocalization analysis for the selected region displayed on the right. F. Quantitative colocalization analysis as a histogram.

FIGURE 7. NLS domain of L-periaxin plays a central role in Schwann cells

Figure 1

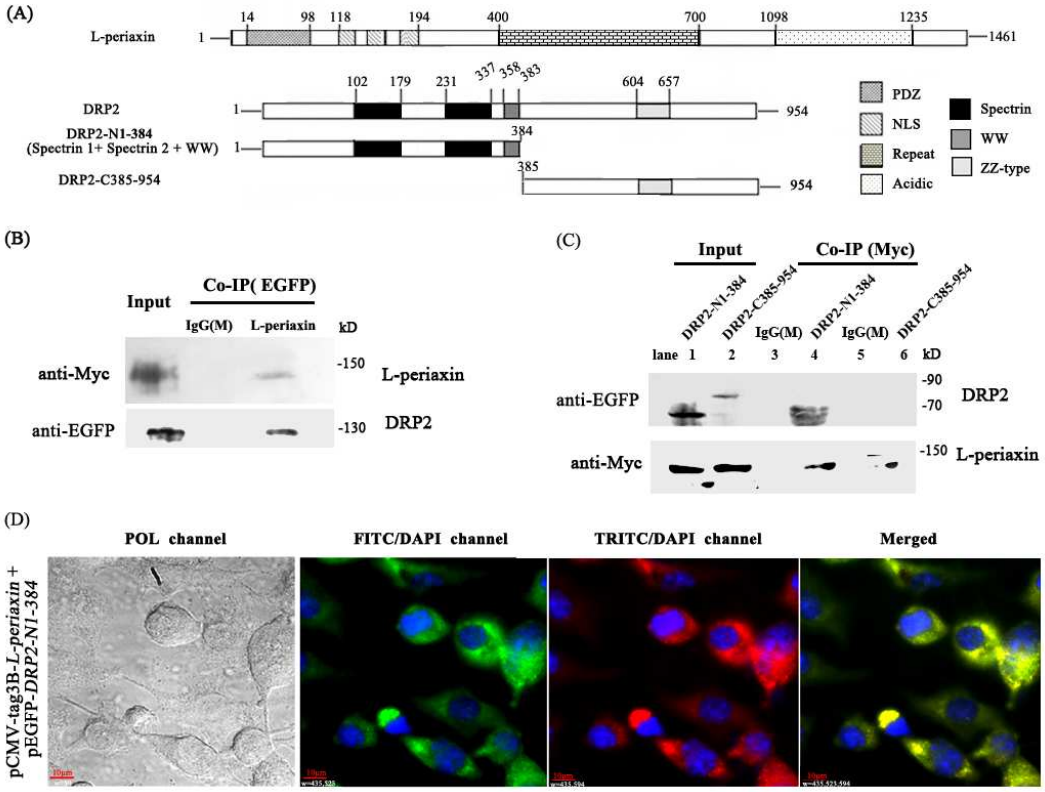

Figure 2

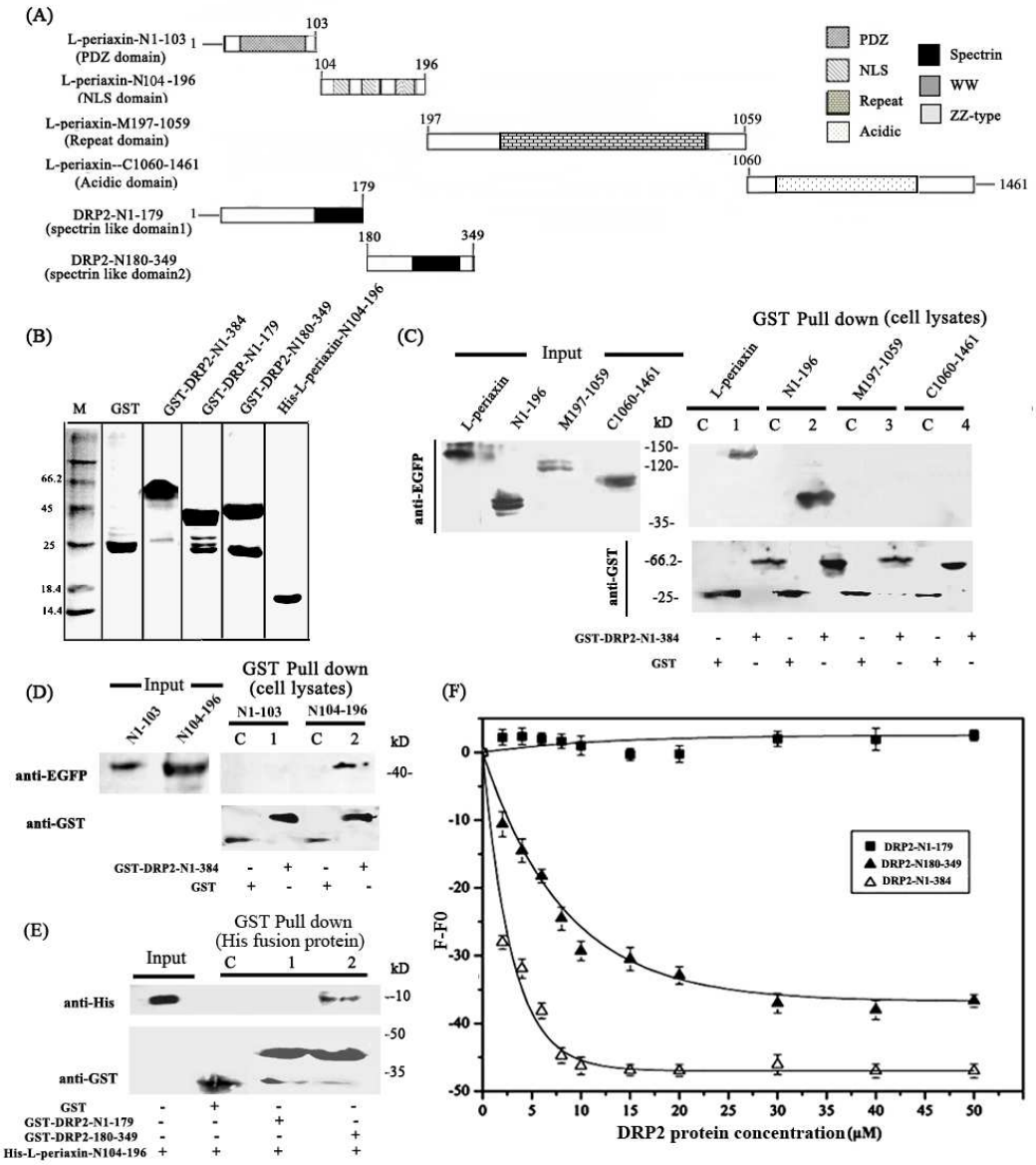

148 **Figure 3**

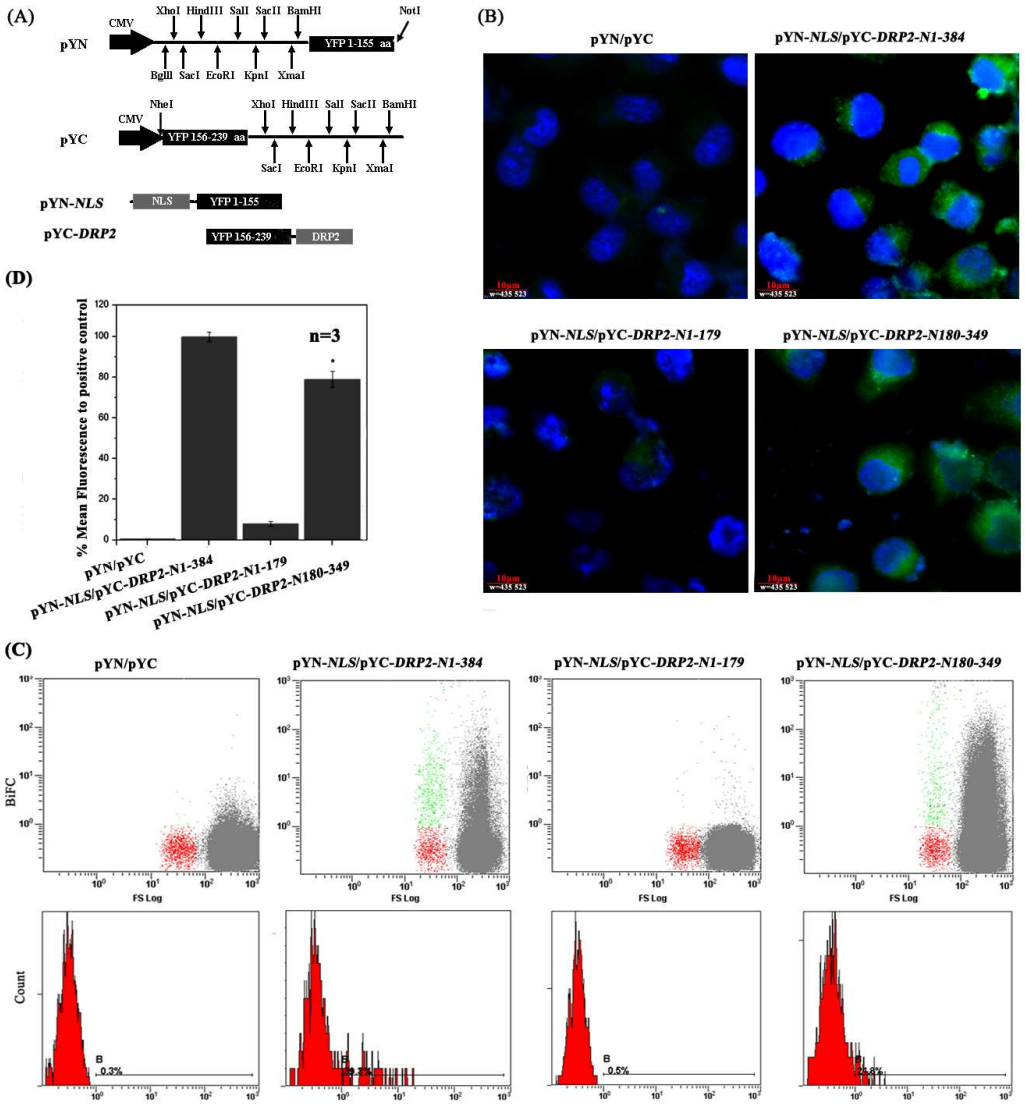

149
150

Figure 4

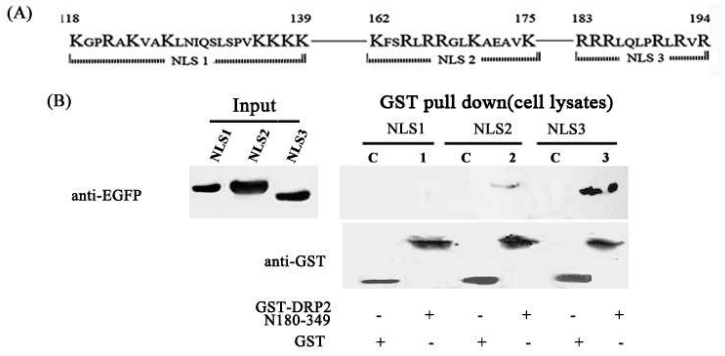

Figure 5

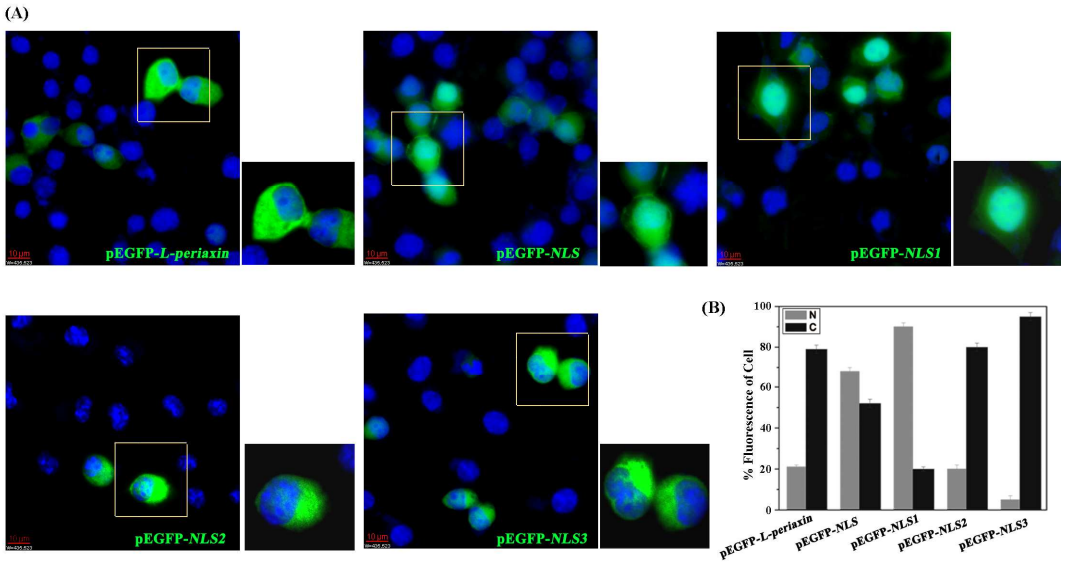

159 **Figure 6**
160

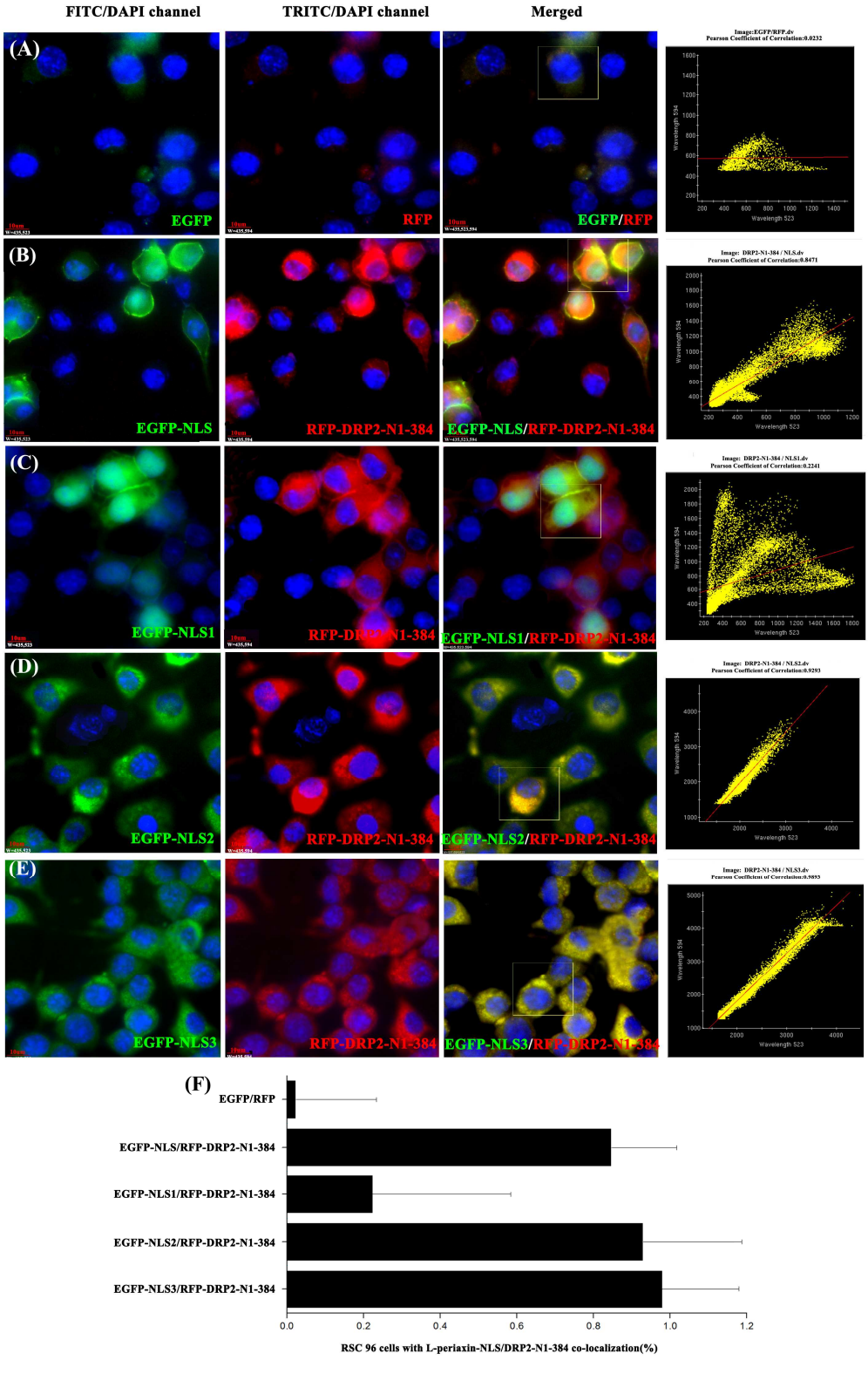

161
162

163 **Figure 7**

164

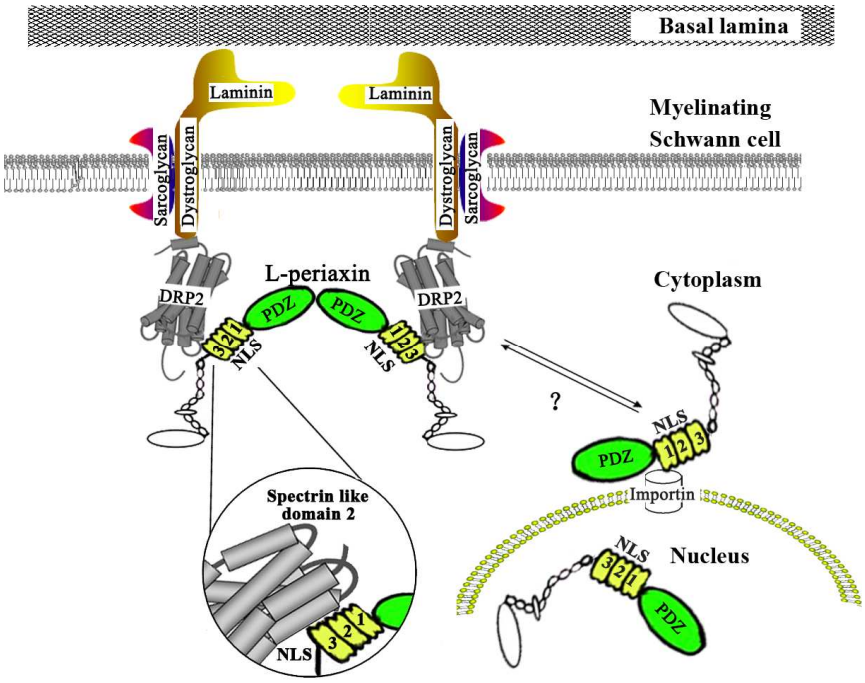

165